A magnetic nozzle calculation of the force on a plasma

A. Fruchtman, K. Takahashi, C. Charles, and R. W. Boswell

Citation: Phys. Plasmas **19**, 033507 (2012); doi: 10.1063/1.3691650
View online: http://dx.doi.org/10.1063/1.3691650
View Table of Contents: http://pop.aip.org/resource/1/PHPAEN/v19/i3
Published by the American Institute of Physics.

A magnetic nozzle calculation of the force on a plasma

A. Fruchtman,[1] K. Takahashi,[2,3] C. Charles,[2] and R. W. Boswell[2]
[1]*Faculty of Sciences, H.I.T. - Holon Institute of Technology, Holon 58102, Israel*
[2]*Space Plasma, Power and Propulsion Group, Research School of Physics and Engineering, The Australian National University, Canberra ACT 0200, Australia*
[3]*Department of Electrical Engineering and Computer Science, Iwate University, Morioka 020-8551, Japan*

(Received 23 November 2011; accepted 7 February 2012; published online 9 March 2012)

The measured axial force imparted from a magnetically expanding current-free plasma has been shown recently [Takahashi, Phys. Rev. Lett. **107**, 235001 (2011)] to equal the axial force on that plasma calculated by a two-dimensional fluid model. Here, we calculate the same axial force on the plasma by a quasi one-dimensional model of a magnetic nozzle. The quasi one-dimensional magnetic nozzle model provides us with an estimate of the force on the plasma that is similar to that found by the more accurate two-dimensional model. © *2012 American Institute of Physics*. [http://dx.doi.org/10.1063/1.3691650]

I. INTRODUCTION

The delivery of momentum to plasma by magnetic field pressure is a dominant process in astrophysical jets,[1] magnetospheric physics,[2] thermonuclear fusion devices,[3] pulsed plasma configurations,[4,5] and electric propulsion devices.[6,7] Recently, the thrust delivered by a plasma jet exiting a plasma source is being considered for space propulsion.[8–12] The thrust may result from the plasma pressure[13] that may be increased due to the formation of a double layer.[14,15] The thrust is substantially larger when the plasma exiting the source flows along a divergent magnetic field because of the additional contribution of the magnetic field pressure in the magnetic nozzle.[16–20] Indeed, the increased thrust of a plasma that flows along a divergent magnetic field has been recently measured.[21] The thrust should be equal in magnitude and opposite in direction to the force exerted on the exiting plasma. Calculations of the two separate contributions to the force on the exiting plasma, that of the plasma pressure[21,22] and that of the magnetic field pressure,[21] have been found to be in a remarkable good agreement with the measurements. In that calculation, the plasma was assumed to be attached to the magnetic field lines.[21] This is a reasonable assumption since, at the location of maximum magnetic field inside the source, the electron and ion Larmor radii are only 0.5 mm and 3 cm, respectively, smaller than the source radius. As plasma accelerates and the magnetic field weakens downstream, plasma detaches from the magnetic field.[23–25]

The calculation of the thrust in Ref. 21 was based on the two-dimensional dependence of the magnetic field and of the internal diamagnetic currents in the plasma. Our purpose here is to make further approximations that allow us to estimate the thrust by a simple quasi one-dimensional model. For the simplified calculation, we follow Ref. 17, in which the paraxial approximation was used, the axial component of the magnetic field is assumed uniform across the radial cross section of the plasma beam. The curved magnetic field lines in the magnetic nozzle then replace the curved physical wall of a nozzle. Although the thrust found through the simplified calculation here is less accurate than that found in the more detailed calculation,[21] the calculation is easier to perform and the analogy to the physical nozzle provides further insight into the physics. We also derive, within the paraxial approximation and with further assumptions, expressions for the axial profiles of the plasma beam density and velocity and of the plasma potential. These calculated profiles will be compared with the experiment in Ref. 21, once additional needed measurements are completed.

In Sec. II, we derive the approximate quasi one-dimensional model and an approximate expression for the thrust. In Sec. III, we compare the thrust calculated by the quasi one-dimensional model to that found in the two-dimensional model.[21] In Sec. IV, we present approximate expressions for the plasma density and velocity and for the plasma potential.

II. THE QUASI ONE-DIMENSIONAL MODEL

Here, we derive the quasi one-dimensional model for the calculation of the thrust. The plasma expands along z in a cylindrical geometry in which the variables are independent of θ. As in Ref. 21, we write the steady-state momentum equations for the electrons

$$-en(E_r + v_\theta B_z) = \frac{\partial p_e}{\partial r}, \quad -en(E_z - v_\theta B_r) = \frac{\partial p_e}{\partial z}, \tag{1}$$

and for the ions,

$$\begin{aligned} en(E_r + u_\theta B_z) &= 0, \\ en(E_z - u_\theta B_r) - F_z &= \frac{1}{r}\frac{\partial}{\partial r}(rmnu_r u_z) + \frac{\partial}{\partial z}(mnu_z^2), \end{aligned} \tag{2}$$

in which $\vec{B}$ is the applied magnetic field and $\vec{E}$ is the ambipolar electric field, both having z and r components only. Also, $\vec{u}$ and $\vec{v}$ are the ion and electron velocities, n is the density of the quasineutral plasma, m is the ion mass and e is the elementary charge. We assume an isotropic electron pressure p_e and neglect the ion pressure. When supersonic rotation is induced, the centripetal force can be important,[26] a case we

do not treat here. The drag on the ions due to collisions with neutral atoms is

$$F_z = mnu_z\nu, \tag{3}$$

where ν is the ion-neutral collision frequency. The axial component of the momentum equation of the neutral gas is

$$F_z = \frac{1}{r}\frac{\partial}{\partial r}(rmNU_rU_z) + \frac{\partial}{\partial z}(mNU_z^2), \tag{4}$$

where N is the neutral-gas density, and U_r and U_z are the components of the neutral-gas velocity. The neutral-gas pressure is neglected in Eq. (4).

Adding Eqs. (1) and (2), we obtain the two components of the one-fluid momentum equation for the plasma,

$$en(u_\theta - v_\theta)B_z = \frac{\partial p_e}{\partial r} \tag{5}$$

and

$$en(v_\theta - u_\theta)B_r = \frac{1}{r}\frac{\partial}{\partial r}(rmnu_ru_z) + \frac{\partial}{\partial z}(mnu_z^2 + p_e) + F_z. \tag{6}$$

We use Eq. (5) to express the azimuthal current as $en(u_\theta - v_\theta) = (1/B_z)\partial p_e/\partial r$ which we substitute into Eq. (6) to obtain

$$-\frac{B_r}{B_z}\frac{\partial p_e}{\partial r} = \frac{1}{r}\frac{\partial}{\partial r}(rmnu_ru_z) + \frac{\partial}{\partial z}(mnu_z^2 + p_e) + F_z. \tag{7}$$

We note that by combining Eqs. (4) and (7), we obtain

$$-\frac{B_r}{B_z}\frac{\partial p_e}{\partial r} = \frac{1}{r}\frac{\partial}{\partial r}(rmnu_ru_z + rmNU_rU_z) + \frac{\partial}{\partial z}(mnu_z^2 + p_e + mNU_z^2), \tag{8}$$

which is a momentum equation for the plasma-neutral gas fluid. Note that the drag term does not change the form of the thrust. The collisions between ions and neutrals are an internal force and only the magnetic field pressure [the LHS of Eq. (8)] imparts momentum to the plasma-neutral gas fluid. Therefore, the drag due to ion-neutral collisions does not enter the calculation of the thrust in the rest of this section.

Integrating the last equation across the cross section of the beam, we obtain an equation for the total T, the total axial force on the plasma-neutral gas flow,

$$T_{total} \equiv \int_0^{r_p(z)} (mnu_z^2 + p_e + mNU_z^2)2\pi r dr, \tag{9}$$

where $r_p(z)$ is the radius of the plasma. As stated above, the thrust delivered by the plasma should be equal in magnitude and opposite in direction to that total force, and we, therefore, relate to T also as the thrust. The equation is

$$\frac{\partial}{\partial z}T_{total} = -\int_0^{r_p(z)} \frac{B_r}{B_z}\frac{\partial p_e}{\partial r}2\pi r dr. \tag{10}$$

The first term on the right hand-side (RHS) of Eq. (8) vanishes in the integration across the plasma radial cross section.

In Ref. 21, the thrust was found through the solution of Eq. (10) with the measured p_e and with B_z and B_r provided by a full two-dimensional code. As in Ref. 21, we write the total thrust as a sum of two contributions

$$T_{total} = T_s + T_B. \tag{11}$$

In the region in which the magnetic field lines do not diverge, the thrust is due to the electron pressure only (which results in a force on the backwall of the plasma source),[27]

$$T_s = \int_0^{r_p(z_0)} p_e(z_0, r)2\pi r dr, \tag{12}$$

and $r_p(z_0)$ is the plasma source radius. Where the magnetic field diverges, the thrust due to the magnetic field pressure increases along z and is written as

$$T_B(z) = -\int_{z_0}^{z} dz' \int_0^{r_p(z)} \frac{B_r}{B_z}\frac{\partial p_e}{\partial r}2\pi r dr. \tag{13}$$

Since the magnetic field is divergence-free, $\vec{\nabla}\cdot\vec{B} = 0$, we write

$$\frac{1}{r}\frac{\partial(rB_r)}{\partial r} + \frac{\partial B_z}{\partial z} = 0, \tag{14}$$

and we obtain, upon integrating Eq. (10) by parts,

$$\frac{\partial}{\partial z}T_{total} = -\int_0^{r_p(z)} \frac{1}{B_z}\frac{\partial B_z}{\partial z}p_e 2\pi r dr + \int_0^{r_p(z)} B_r\frac{\partial(1/B_z)}{\partial r}p_e 2\pi r dr. \tag{15}$$

The contribution of $(B_r/B_z)p_e 2\pi r$ is zero both on axis (where B_r is zero) and at the radial boundary of the plasma (where p_e is zero). We are now making the paraxial approximation,

$$B_z(r, z) \cong B_z(0, z). \tag{16}$$

We neglect the second term on the RHS of Eq. (15), so that the simplified equation becomes

$$\frac{\partial}{\partial z}T_{total,p} = -\frac{1}{B_z}\frac{\partial B_z}{\partial z}\langle p_e\rangle A(z), \tag{17}$$

where

$$A(z) = \pi r_p^2(z) \tag{18}$$

is the radial cross section of the plasma and $\langle p_e\rangle$ is the radially-averaged plasma pressure,

$$\langle p_e\rangle(z) \equiv \frac{1}{A(z)}\int_0^{r_p(z)} p_e(z, r)2\pi r dr. \tag{19}$$

The subscript p in $T_{total,p}$ denotes the paraxial approximation. We note that in the form of the paraxial approximation used

here, the details of the radial profile of the plasma pressure do not affect the thrust. The plasma pressure affects the thrust through the integral in Eq. (19) only. The effect of the pressure radial profile should be studied within a higher-order paraxial approximation or within the two-dimensional fluid model.[21]

Equation (17) can be used for the calculation of the contribution of the magnetic field. Inside the plasma source, the plasma radius is constant, $r_p(z)$ equal r_s, the plasma source radius, and Eq. (17) becomes

$$\frac{\partial}{\partial z}T_{total,p} = -\frac{1}{B_z}\frac{\partial B_z}{\partial z}\langle p_e\rangle A_{exit}, \tag{20}$$

where $A_{exit} = \pi r_s^2$ is the cross-section area of the plasma source. Thrust is lost when energetic ions, which are accelerated towards the source exit, recombine with electrons while impinging on (or, for certain ion species,[28] are implanted into) lateral walls. We assume here that due to the confining magnetic field, neither ions nor neutral atoms lose momentum in their collisions with the lateral walls.

Let us assume that once it exits the source tube, the plasma flow is attached to the magnetic field lines. This assumption was also made in Ref. 21, although without the paraxial approximation. We, therefore, write

$$\langle p_e\rangle(z) = \frac{B_z(z)}{\Phi_0}\int_0^{r_p(z)} p_e(z,r)2\pi r dr, \tag{21}$$

where Φ_0 is the constant in z magnetic field flux,

$$\Phi_0 \equiv B_z(z)A(z) = B_{exit}A_{exit}. \tag{22}$$

Here, B_{exit} is the magnetic field intensity at the exit from the plasma source. We can write the equation for the thrust as

$$\frac{\partial}{\partial z}T_{total,p} = \Phi_0\frac{\partial}{\partial z}\left(\frac{1}{B_z}\right)\langle p_e\rangle, \tag{23}$$

or, in analogy to a physical nozzle,[17] as

$$\frac{\partial}{\partial z}T_{total,p} = \frac{\partial A}{\partial z}\langle p_e\rangle. \tag{24}$$

The contribution to the thrust is the component in the z direction of the force by the "wall" (the magnetic field) that balances the electron pressure.[17] This acceleration is similar in form to the acceleration of a plasma by area expansion without magnetic field pressure.[29,30] We note that Eq. (24) can be interpreted as a force that results from an integration of the pressure across the area,

$$T_{total,p} = \int_{A_i}^{A} dA'\langle p_e\rangle, \tag{25}$$

where A_i is the initial area.

A further assumption is that the electron pressure is of a self similar form, which we describe as in Ref. 21 as

$$p_e(z,r) = p_e(z_0,0)p_{en}(z)f\{[r/r_p(z)]^2\}, \tag{26}$$

where the maximal electron pressure is at $z = z_0$ and $f(0) = 1$. With this form for the electron pressure, the average electron pressure becomes

$$\langle p_e\rangle(z) = p_e(z_0,0)p_{en}(z)f_1, \quad f_1 \equiv \int_0^1 f(\xi)d\xi. \tag{27}$$

The approximated equation for the thrust inside the plasma source is

$$\frac{\partial T_{total,p}}{\partial z} = -A_{exit}f_1 p_e(z_0,0)\frac{1}{B_z}\frac{\partial B_z}{\partial z}p_{en}(z), \tag{28}$$

while the approximated equation for the thrust outside the plasma source is

$$\frac{\partial T_{total,p}}{\partial z} = \Phi_0 f_1 p_e(z_0,0)\frac{\partial}{\partial z}\left(\frac{1}{B_z}\right)p_{en}(z). \tag{29}$$

The contribution to the thrust by the electron pressure upstream is

$$T_s = \langle p_e\rangle(z_0)\pi r_p^2(z_0), \tag{30}$$

which, with the use of the form in Eq. (26), becomes

$$T_s = f_1 p_e(z_0,0). \tag{31}$$

The contribution to the thrust by the magnetic field pressure is obtained from Eq. (10) as

$$T_{B,f} = -p_e(z_0,0)\int_{z_0}^{z} dz' p_{en}(z')\int_0^{r_p(z')}\frac{B_r}{B_z}\frac{\partial f}{\partial r}2\pi r dr. \tag{32}$$

The subscript f in $T_{B,f}$ denotes that this is the thrust found through a full calculation without the use of Eq. (16), the paraxial approximation for the magnetic field. Within the paraxial approximation, the contribution to the thrust of the magnetic field pressure becomes

$$T_{B,p}(z) = f_1 p_e(z_0,0)\left[-A_{exit}\int_{z_0}^{0}\frac{1}{B_z}\frac{\partial B_z}{\partial z}p_{en}(z)dz + \Phi_0\int_0^z\frac{\partial}{\partial z'}\left(\frac{1}{B_z}\right)p_{en}(z')dz'\right]. \tag{33}$$

which can also be written formally as

$$T_{B,p}(z) = f_1 p_e(z_0,0)\left[-A_{exit}\int_{\ln(B_{z_0})}^{\ln(B_{exit})} d(\ln B_z)p_{en}(\ln B_z) + \int_{A_0}^{A} dA' p_{en}(A')\right]. \tag{34}$$

The two last expressions were obtained from Eqs. (28) and (29). The subscript p in $T_{B,p}$ denotes that this is the thrust found within the paraxial approximation.

In Sec. III, we compare $T_{B,f}$ and $T_{B,p}$ for the experiment described in Ref. 21.

III. COMPARISON OF THE CALCULATIONS BY THE TWO MODELS

The experiment is described in Ref. 21 and consists in measuring the thrust T_B resulting from the magnetic field pressure in a 1 mTorr argon radiofrequency (13.56 MHz) plasma for two distinct magnetic field configurations shown on Figures 1(a) and 1(b) (where z = 0 cm is defined as the open end of the cylindrical plasma cavity and the start of the expansion). Briefly, a 25-cm-long, 9-cm-diameter plasma source with an expanding magnetic field created using two axial solenoids positioned around the source (Fig. 1(b)) is immersed in a 140-cm-long, 50-cm-diameter vacuum vessel. The two loop rf antenna surrounding the cavity is centered at z = −12 cm and the gas inlet is located at the closed end of the source. The two solenoids are suspended to a grounded thrust balance equipped with a laser/sensor system to measure the axial force T_B as a function of rf power for the two magnetic field configurations: Mode A corresponds to a current of 6 A in each solenoid (left pane of Fig. 1(b)) and Mode B corresponds to a current of 6 A in the solenoid closest to the source exit only (right pane of Fig. 1(b)).

The function $p_{en}(z)$ obtained by direct measurements using a Langmuir probe is shown for the two modes in Fig. 2. Also, as in Ref. 21, the pressure profile is described by choosing the function f in Eq. (26) to be of the form,

$$f(\xi) = 1 - \xi^{(a_1/2)}, \quad \xi \le 1, \tag{35}$$

for mode A and

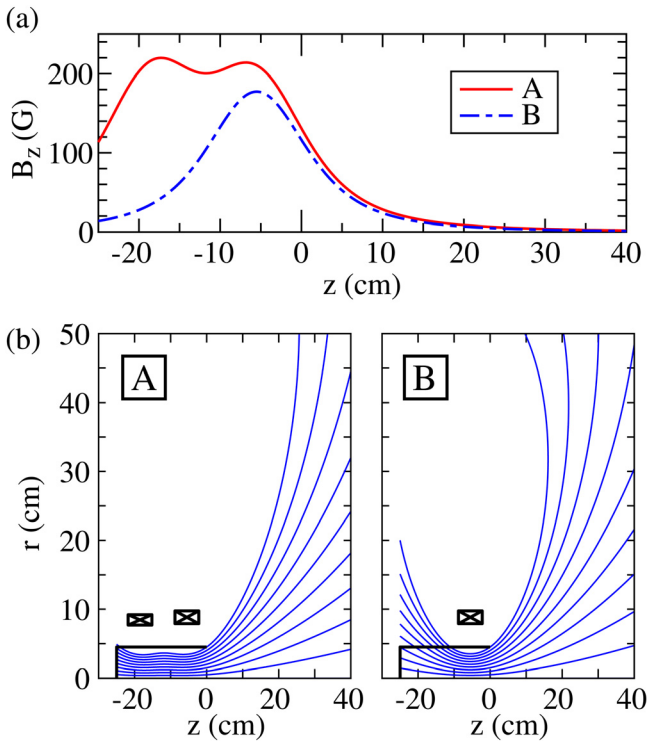

FIG. 1. (Color online) (a) Axial profiles of the magnetic field B_z on axis and (b) topologies of the magnetic field lines, for modes A and B. The position of the radial wall of the outer chamber is at r = 50 cm.

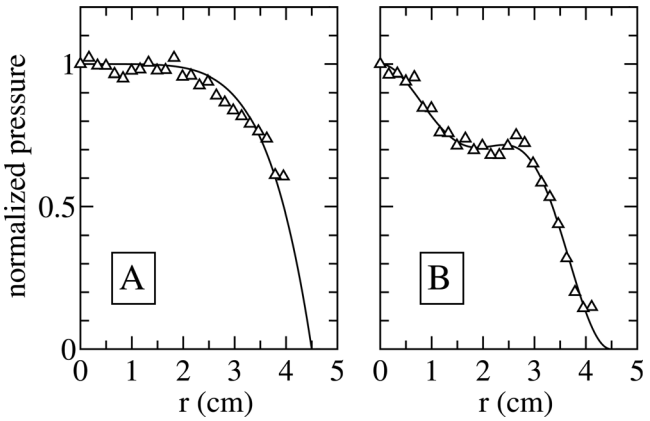

FIG. 2. Normalized pressure f and p_{en}, for modes A and B.

$$f(\xi) = a_2[1 - \xi^{(a_1/2)}]^{a_3} + (1 - a_2)[1 - \xi^{(a_4/2)}]^{a_5}, \quad \xi \le 1, \tag{36}$$

for mode B. For both modes, $f(\xi) = 0$ for $\xi > 1$. The constants $a_1 - a_5$ are fitting parameters of the electron pressure radial profiles measured at z_0. Figure 2 also shows the measured and fitted radial profiles of the normalized electron pressure $f(\xi)$ for modes A and B. The maximum electron pressure $p_e(z_0, 0)$, measured for various values of radiofrequency power, is used for the calculation, and is not shown here.

Figure 3 shows $T_{B,f}$ and $T_{B,p}$ for the two modes as functions of the rf power, calculated through Eqs. (32) and (33) at $z = 40$ cm. It was shown in Ref. 21 that there is a good agreement between the calculated $T_{B,f}$ and the measured contribution of the magnetic field pressure to the thrust. It should be noted that there is an order of magnitude difference between the T_B values obtained for Mode A and Mode B which results from much lower values of $p_{en}(z)$ downstream of the plasma source for Mode A.[21] The agreement between the calculated thrust at $z = 40$ cm and the measured thrust[21] indicates that no thrust is delivered beyond that

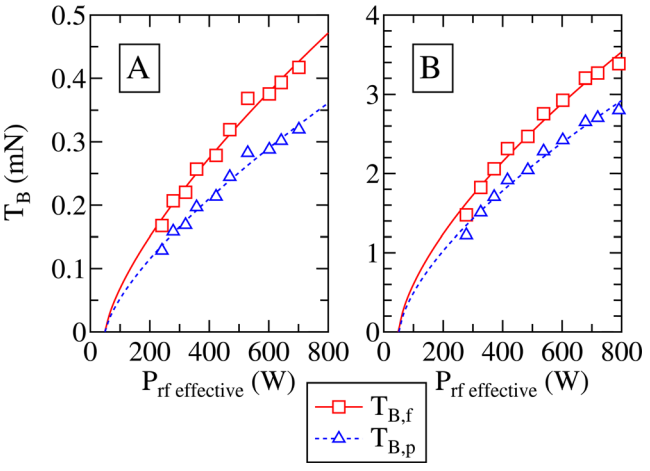

FIG. 3. (Color online) The thrust at $z = 40$ cm versus the wave power, as calculated by the two-dimensional model and in the paraxial approximation, for modes A and B. The largest contribution to the thrust in mode B is from regions in which B_z is more uniform radially, resulting in the magnetic nozzle model to be more accurate for that mode.

point, probably due to plasma detachment from the magnetic field lines.

The calculation within the paraxial approximation is easier and the analogy to a nozzle is useful. The numerical results in Fig. 3 exhibit the power as well as the limitations of the magnetic nozzle model. Over the range of power investigated here (200–800 W), the ratio between the approximate calculated thrust $T_{B,p}$ (dotted line on Fig. 3) and the more accurate calculated thrust $T_{B,f}$ (solid line on Fig. 3) is constant, about 0.76 for mode A and about 0.83 for mode B. The discrepancy between the calculated thrust by the two models originates from the approximation in the magnetic nozzle model that B_z across the cross section of the plasma is independent of r. When the largest contribution to the thrust is from regions in which B_z is more uniform radially, as it is in mode B, the paraxial approximation results are more accurate.

In Sec. IV, we calculate, within further assumptions, the axial profiles of the plasma density and velocity.

IV. AXIAL PROFILES OF PLASMA DENSITY AND VELOCITY

In this section, we calculate the axial profiles of the plasma density and velocity while the plasma expands along magnetic field lines outside the plasma source. Combining Eq. (7), integrated across the beam, and Eq. (23), we write, within the paraxial approximation, that

$$\Phi_0 \frac{\partial}{\partial z}\left(\frac{1}{B_z}\right)\langle p_e\rangle = \frac{\partial}{\partial z}\int_0^{r_p(z)} (mnu_z^2 + p_e)2\pi r dr + \int_0^{r_p(z)} F_z 2\pi r dr, \tag{37}$$

which is analogous to Eq. (4) in Ref. 17. This equation is easily transformed into

$$0 = \frac{\partial}{\partial z}\int_0^{r_p(z)} mnu_z^2 2\pi r dr + A\frac{\partial}{\partial z}\langle p_e\rangle + \int_0^{r_p(z)} F_z 2\pi r dr. \tag{38}$$

We now assume that u_z and the electron temperature T_{el} are approximately constant across the plasma,

$$u_z(z,r) \cong u_z(z), \quad T_{el}(z,r) \cong T_e(z). \tag{39}$$

We further assume that ν is constant across the radial cross-section of the plasma. The momentum equation is approximated as

$$0 = m\frac{\partial}{\partial z}(\Gamma u_z) + A\frac{\partial}{\partial z}(T_e\langle n\rangle) + m\Gamma\nu, \tag{40}$$

where

$$\Gamma \equiv \int_0^{r_p(z)} nu_z 2\pi r dr, \tag{41}$$

is the plasma particle flux, which is expressed as

$$\Gamma = n_z(z)u_z(z), \quad n_z(z) \equiv A\langle n\rangle, \tag{42}$$

and we used

$$\langle p_e\rangle = T_e\langle n\rangle. \tag{43}$$

Within this hydrodynamic analogy, we write the equation with the independent variable A [$= B_{exit}A_{exit}/B_z$, according to Eq. (22)]. Equation (40) becomes

$$0 = \frac{\partial}{\partial A}(\Gamma u_z) + A\frac{\partial}{\partial A}\left(\frac{c^2\Gamma}{Au_z}\right) + \frac{\partial z}{\partial A}\Gamma\nu, \tag{44}$$

where

$$c^2 \equiv \frac{T}{m} \tag{45}$$

is the square of the ion acoustic velocity. This equation is written now as

$$(M^2-1)\frac{\partial \ln M}{\partial \ln A} = 1 - (M^2+1)\frac{\partial \ln(\Gamma c)}{\partial \ln A} - \frac{\partial z}{\partial \ln A}\frac{M\nu}{c}, \tag{46}$$

where

$$M \equiv \frac{u_z}{c} \tag{47}$$

is the plasma Mach number.

If the electron temperature does not change along the plasma flow, ionization is small, and there are no collisions, all except for the first term on the RHS of Eq. (46) vanish. The plasma accelerates along the divergent magnetic field if the flow is supersonic $M \geq 1$. Integrating Eq. (46) for constant c and Γ and $\nu = 0$, we obtain the following relation between the plasma Mach number and the magnetic field intensity:

$$\frac{M^2 - M_i^2}{2} - \ln\left(\frac{M}{M_i}\right) = \ln\left(\frac{A}{A_i}\right) = \ln\left(\frac{B_{zi}}{B_z}\right). \tag{48}$$

Here, $M = M_i$, when $B_z = B_{zi}$. The subscript i denotes that this is the value of the quantity at the boundary, where the calculation begins. Equivalently to a nozzle, there is a monotonic increase of the M with a decrease of B_z for $M > 1$, the supersonic regime, and with an increase of B_z for $M < 1$, the subsonic regime.

Let us examine an interesting effect that ion-neutral collisions may have. We now assume that ν is not zero, while c and Γ are constant. In order to illustrate the effect, let us choose $A = A_i(z/z_i)$ and a not-so-realistic collision frequency of the form $\nu = \nu_1 c/z_i M$, in which ν_1 is a constant. Equation (46) becomes $(M^2-1)\partial \ln M/\partial \ln A = 1 - \nu_1(A/A_i)$, and its solution, for $M_i = 1$, is

$$\frac{M^2-1}{2} - \ln M = \ln\left(\frac{z}{z_i}\right) - \nu_1\left(\frac{z}{z_i} - 1\right) = \ln\left(\frac{B_{zi}}{B_z}\right) - \nu_1\left(\frac{B_{zi}}{B_z} - 1\right). \tag{49}$$

It is clear that M is not monotonic, it first increases along the decreasing magnetic field but then decreases. Accordingly,

$n_z(z)$ first decreases and then increases. We note that in reality, ν is not expected to decrease as M increases, as we assumed here. If ν does not decrease as M increases, the nonmonotonic behavior of M, predicted here, should be even more apparent.

Let us examine which of Eq. (48) or Eq. (49) better describes the experiment detailed in Ref. 21. If the ion velocity increases monotonically along the divergent magnetic field, while the plasma flux is constant, the density per unit length, n_z [Eq. (42)],

$$n_z = \frac{\Gamma}{cM}, \tag{50}$$

should decrease accordingly. However, measurements of the plasma density in the experiments described in Ref. 21 show that n_z does not decrease and even slightly increases along the divergent magnetic field. The existence of a regime of an increasing density suggests the possibility that ion-neutral collisions do decelerate the ions, as illustrated by Eq. (49).

Let us now discuss the axial potential profile. We assume that the ion rotation is small and that E_z is approximately uniform across the plasma radial cross section. Integrating across r, we obtain that the ions satisfy

$$eE_z - mu_z\nu \cong mu_z\frac{\partial u_z}{\partial z} \Rightarrow \frac{e(\varphi_i-\varphi)}{T_e} - \int_{z_i}^{z} mu_z\nu dz' = \frac{M^2-M_i^2}{2}. \tag{51}$$

If we use again the assumptions that $A = A_i(z/z_i)$ and that $\nu = \nu_1 c/z_i M$, we obtain that

$$eE_z - mu_z\nu \cong mu_z\frac{\partial u_z}{\partial z} \Rightarrow \frac{e(\varphi_i-\varphi)}{T_e} - \nu_1\left(\frac{z}{z_i}-1\right) = \frac{M^2-M_i^2}{2}. \tag{52}$$

Although the plasma potential is measured to decrease along the divergent magnetic field, the ions may decelerate due to the ion-neutral collisions, which, according to Eq. (50), will result in an increase of n_z along the divergent magnetic field.

The increase of the plasma density n_z along the divergent magnetic field could result from other reasons. It could be that there is further ionization downstream. The density n_z then increases according to Eq. (50) even though M increases because Γ increases as well. The plasma dynamics in the experiments in the configuration described in Ref. 21 will be further studied in future studies. It will be examined whether ion-neutral collisions or ionization is the source of the plasma density increase downstream.

V. SUMMARY

We have applied a simple model based on the paraxial approximation[17] to a plasma that flows out of a plasma source along a divergent magnetic field.[21] The simple model, a quasi one-dimensional model of a magnetic nozzle, enabled us to calculate the momentum delivered to the plasma by the magnetic field with a good accuracy, although a more detailed two-dimensional model has achieved a higher accuracy.[21] The magnetic nozzle model can, therefore, be used in experiments for a quick and simple estimate of the thrust by the measured axial magnetic field on axis. When radial variations of the magnetic field are significant, a higher-order paraxial approximation could be employed or one could resort to a calculation that uses a full mapping of the magnetic field across the plasma beam.

We also used the magnetic nozzle model to solve for the axial profiles of the plasma density and velocity. Further measurements are needed for testing the predictions of the model.

ACKNOWLEDGMENTS

This research has been partially supported by the Israel Science Foundation (Grants 864/07 and 765/11).

[1]D. L. Meier, S. Koide, and Y. Uchida, Science **291**, 84 (2001).
[2]T. E. Eastman, Geophys. Res. Lett. **3**, 685,doi: 10.1029/GL003i011p00685 (1976).
[3]A. G. Peeters, C. Angioni, and D. Strintzi, Phys. Rev. Lett. **98**, 265003 (2007).
[4]R. Arad, K. Tsigutkin, Y. Maron, and A. Fruchtman, Phys. Plasmas **11**, 4515 (2004).
[5]M. G. Haines, Plasma Phys. Controlled Fusion **53**, 093001 (2011).
[6]M. Martinez-Sanchez and J. E. Pollard, J. Propul. Power **14**, 688 (1998).
[7]M. Zuin, R. Cavazzana, E. Martines, G. Serianni, V. Antoni, M. Bagatin, M. Andrenucci, F. Paganucci, and P. Rossetti, Phys. Rev. Lett. **92**, 225003 (2004).
[8]C. Charles, J. Phys. D: Appl. Phys. **42**, 163001 (2009).
[9]O. V. Batishchev, IEEE Trans. Plasma Sci. **3**, 1563 (2009).
[10]S. Shinohara, T. Hada, T. Motomura, K. Tanaka, T. Tanikawa, K. Toki, Y. Tanaka, and K. P. Shamrai, Phys. Plasmas **16**, 057104 (2009).
[11]A. W. Kieckhafer and M. L. R. Walker, Rev. Sci. Instrum. **81**, 75 (2010).
[12]S. Pottinger, V. Lappas, C. Charles, and R. Boswell, J. Phys. D: Appl. Phys. **44**, 235201 (2011).
[13]A. Fruchtman, IEEE Trans. Plasma Sci. **36**, 403 (2008).
[14]C. Charles and R. Boswell, Appl. Phys. Lett. **82**, 1356 (2003).
[15]X. Sun, A. M. Keesee, C. Biloiu, E. E. Scime, A. Meige, C. Charles, and R. W. Boswell, Phys. Rev. Lett. **95**, 025004 (2005).
[16]A. Sasoh, Phys. Plasmas **1**, 464 (1994).
[17]A. Fruchtman, Phys. Rev. Lett. **96**, 065002 (2006).
[18]H. Tobari, A. Ando, M. Inutake, and K. Hattori, Phys. Plasmas **14**, 093507 (2007).
[19]E. Ahedo and M. Merino, Phys. Plasmas **17**, 073501 (2010).
[20]B. W. Longmier, E. A. Bering III, M. D. Carter, L. D. Cassady, W. J. Chancery, F. C. Díaz, T. W. Glover, N. Hershkowitz, A. V. Ilin, G. E. McCaskill, C. S. Olsen, and J. P. Squire, Plasma Sources Sci. Technol. **20**, 015007 (2011).
[21]K. Takahashi, T. Lafleur, C. Charles, P. Alexander, and R. W. Boswell, Phys. Rev. Lett. **107**, 235001 (2011).
[22]K. Takahashi, T. Lafleur, C. Charles, P. Alexander, R. W. Boswell, M. Perren, R. Laine, S. Pottinger, V. Lappas, T. Harle, and D. Lamprou, Appl. Phys. Lett. **98**, 141503 (2011).
[23]E. B. Hooper, J. Propul. Power **9**, 757 (1993).
[24]A. V. Arefiev and B. N. Briezman, Phys. Plasmas **12**, 043504 (2005).
[25]P. F. Schmit and N. J. Fisch, J. Plasma Phys. **75**, 359 (2009).
[26]N. J. Fisch, Y. Raitses, and A. Fruchtman, Plasma Phys. Controlled Fusion **53**, 124038 (2011).
[27]T. Lafleur, K. Takahashi, C. Charles, and R. W. Boswell, Phys. Plasmas **18**, 080701 (2011).
[28]B. Longmier, A. Gallimore, F. C. Diaz, J. Squire, G. Chavers, T. Glover, E. Bering III, and B. Ried, J. Propul. Power **25**, 746 (2009).
[29]A. Fruchtman, N. J. Fisch, and Y. Raitses, Phys. Plasmas **8**, 1048 (2001).
[30]W. M. Manheimer and R. F. Fernsler, IEEE Trans. Plasma Sci. **29**, 75 (2001).